Talanta 83 (2011) 1068–1073

Contents lists available at ScienceDirect

Talanta

journal homepage: www.elsevier.com/locate/talanta

Dependence on effective saturation of numbers of singlet peaks in one- and two-dimensional separations

Joe M. Davis*

Department of Chemistry and Biochemistry, Southern Illinois University at Carbondale, Carbondale, IL 62901 USA

ARTICLE INFO

Keywords:
Effective saturation
Singlet
Statistical-overlap theory

ABSTRACT

The average numbers of singlet peaks in one-dimensional (1D) and two-dimensional (2D) separations of randomly distributed peaks are predicted by statistical-overlap theory and compared against the effective saturation. The effective saturation is a recently introduced metric of peak crowding that is more practitioner-friendly than the usual metric, the saturation. The effective saturation absorbs the average minimum resolution of statistical-overlap theory, facilitating the comparison of 1D and 2D separations by traditional metrics of resolution and peak capacity. In this paper, singlet peaks are identified with maxima produced by a single mixture constituent. Their effective saturations are calculated from published equations for the average minimum resolution of 1D singlet peaks, and from equations derived here for the average minimum resolution of 2D singlet peaks. The fractions of peaks that are singlets in 1D and 2D separations are predicted by statistical-overlap theory as functions of saturation but are compared as functions of effective saturation. The two fractions differ by no more than 0.033 at any effective saturation between 0 and 6, when the distribution of peak heights is exponential and the edge effect is neglected. This result shows that 1D and 2D separations of randomly distributed peaks are about the same in their ability to separate singlet peaks as maxima, when assessed relative to effective saturation. Empirical equations in effective saturation are reported for the fractions of peaks that are singlets. It is argued that the effective saturation is a good metric for comparing separations having different average minimum resolutions.

1. Introduction

This paper compares the number of singlet peaks in one-dimensional (1D) and two-dimensional (2D) separations of randomly distributed peaks, as predicted by statistical-overlap theory (SOT) and the metric of effective saturation. In SOT, one postulates that the intervals between peaks and the heights of peaks in a large ensemble of separations are governed by probability distributions, from which the average amount of peak overlap in the ensemble can be calculated. Different types of SOT exist and are based on point-process statistics [1–13], pulse-point statistics [14,15], and Fourier analysis [16–21].

The fundamental metric of peak crowding in point-process SOT is the saturation, which (as shown below) depends on the average number of peaks in the separation ensemble, the duration or length of the separation, and the peak standard deviation. It also depends on the average minimum resolution, which relates peak overlap and various metrics of performance (e.g., the SOT-based peak capacity) to the average minimum interval between peaks that is required for separation. However, traditional metrics in separations typically are not scaled to the average minimum interval, and this makes it possible for SOT predictions to be misinterpreted.

For example, one prediction is that at the same saturation the ratio of the average number of observed peaks in the separation ensemble to the average number of peaks in the ensemble is smaller in 2D separations than in 1D ones [6]. Here, a "peak" is the concentration profile of a single mixture constituent produced by a univariate detector (e.g., a single mass channel of a mass spectrometer or single wavelength of a UV spectrophotometer), whereas an "observed peak" is a detected maximum that may contain one or more constituents [22]. Extensive simulation results support the SOT prediction [22]. The prediction was reassessed recently relative to a new metric of peak crowding, the effective saturation [22]. The effective saturation has advantages over saturation because it absorbs the average minimum resolution as an internal attribute, allowing SOT predictions to be referenced to the traditional metrics of resolution and peak capacity used by practitioners. For reasons discussed below, the effective saturations of 1D and 2D separations increase at different rates with increasing saturation, causing SOT predictions to scale differently relative to the two metrics. Relative to the effective saturation, the SOT-predicted ratios of the average

* Permanent address: 733 Schloss Street, Wrightsville Beach, NC 28480, USA. Tel.: +1 910 256 4235.
E-mail address: chimicajmd@ec.rr.com.

0039-9140/$ – see front matter © 2010 Elsevier B.V. All rights reserved.
doi:10.1016/j.talanta.2010.06.040

numbers of observed peaks to peaks are essentially the same in 1D and 2D separations having the same traditional peak capacities, when the traditional resolutions are unity and the 2D space is large compared to the peak widths [22]. From this result, the authors concluded that neither separation type is superior to the other and that the separation having the greater traditional peak capacity (usually the 2D one) should be chosen.

The qualitative and quantitative analysis of 1D and 2D separations is greatly simplified if observed peaks are free of peak overlap, i.e., if they are singlet peaks (or singlets) of a single mixture constituent. Relative to the saturation, SOT predicts that the ratio of the average number of singlets in the separation ensemble to the average number of peaks is smaller in 2D separations than in 1D ones, just as it is for observed peaks [23]. Because the analysis of singlets is so important, it is instructive to know if these ratios differ relative to effective saturation. However, one cannot make this assessment simply by using the same function relating saturation and effective saturation for observed peaks. This is because the average minimum resolution is not a simple metric whose value is invariant. In fact, when observed peaks are maxima, its value depends on the amount of peak overlap [10,13], the dimensionality of separation [10,13], and the type of observed peak (e.g., all observed peaks, singlets, doublet peaks, etc.) [24]. For this assessment, the average minimum resolution of singlets is needed. Although it is known for 1D separations [24], its 2D counterpart must be derived.

A brief comment on terminology is warranted. The terminology of Schoenmakers et al. for multi-dimensional separations is used when possible [25]. Unique symbols for several expressions of probability and resolution are used, with somewhat detailed subscripts and superscripts to distinguish them. Some symbols previously used in SOT are changed for simplicity and internal consistency. The subscripts, 1D and 2D, are assigned to symbols as needed to identify the dimensionality of separation. All symbols are listed in a Glossary at the end of the paper.

2. Theory

2.1. Review of basic equations

Consider a separation of duration or length ${}^1D$ containing peaks of standard deviation ${}^1\sigma$. It either stands alone as a 1D separation, or is coupled to a rectangular 2D separation by a second dimension of duration or length ${}^2D$ containing peaks of standard deviation ${}^2\sigma$. The saturations α_{1D} and α_{2D} of these separations are [3,10,13,26]

$$\alpha_{1D} = \frac{4\bar{m}\,{}^1\sigma\bar{R}_{1D}}{{}^1D} \tag{1}$$

$$\alpha_{2D} = \frac{4\pi\bar{m}\,{}^1\sigma^2\sigma(\bar{R}_{2D})^2}{({}^1D^2D)} \tag{2}$$

where $\bar{m}$ is the average number of peaks (or mixture constituents) in the separation ensemble, and $\bar{R}_{1D}$ and $\bar{R}_{2D}$ are the average minimum resolutions. One interpretation of saturation is the ratio of the average number of peaks to the SOT-based peak capacity, as calculated from the average minimum resolution [3,23]. The saturation increases as peak overlap increases.

In separations of randomly distributed peaks, two important results are the probability p_{1D} of separating two adjacent 1D peaks [3] and the probability p_{2D} of separating a 2D peak from its nearest-neighbor peak [23]

$$p_{1D} = \exp(-\alpha_{1D}) \tag{3}$$

$$p_{2D} = \exp(-4\alpha_{2D}) \tag{4}$$

Eq. (4) is an approximation, which is valid only if the 2D separation is sufficiently large that the increased probability of separation near the boundary (due to the absence of peaks outside the boundary) is negligible. Such separations are designated unbounded. Equations for the probability increase due to this "edge effect" have been published [12].

The average numbers of singlets s_{1D} and s_{2D} in 1D separations and unbounded 2D separations of randomly distributed peaks are simple functions of p_{1D} and p_{2D} [3,5,23]

$$s_{1D} = \bar{m}p_{1D}^2 = \bar{m}\exp(-2\alpha_{1D}) \tag{5}$$

$$s_{2D} = \bar{m}p_{2D} = \bar{m}\exp(-4\alpha_{2D}) \tag{6}$$

The general relations between the saturations α_{1D} and α_{2D}, and their corresponding effective saturations $\alpha_{e,1D}$ and $\alpha_{e,2D}$, are [22]

$$\alpha_{e,1D} = \frac{\alpha_{1D}}{\bar{R}_{1D}} = \frac{\bar{m}}{{}^1R_s\,{}^1n_c} \tag{7}$$

$$\alpha_{e,2D} = \frac{4\alpha_{2D}}{\pi(\bar{R}_{2D})^2} = \frac{\bar{m}}{n_{c,2D}\,{}^1R_s\,{}^2R_s} \tag{8}$$

where ${}^1R_s$ and ${}^2R_s$ are the traditional resolutions of the first and second dimensions of a 2D separation. The former also is the traditional resolution of a 1D separation. The metrics

$${}^1n_c = \frac{{}^1D}{4\,{}^1\sigma\,{}^1R_s} \tag{9a}$$

$${}^2n_c = \frac{{}^2D}{4\,{}^2\sigma\,{}^2R_s} \tag{9b}$$

$$n_{c,2D} = {}^1n_c\,{}^2n_c \tag{9c}$$

are the traditional peak capacities of the first and second dimensions of a 2D separation, and of the entire 2D separation, respectively. Eq. (9a) also is the traditional peak capacity of a 1D separation. The effective saturation, like the saturation, increases as peak overlap increases. Its exact relation to saturation depends on the value of the average minimum resolution. Eqs. (7) and (8) show that if the traditional resolutions are assigned the common value, one, then 1D and 2D separations of the same mixture of $\bar{m}$ constituents have the same traditional peak capacities at the same effective saturation, facilitating a comparison of 1D and 2D separations by SOT that is simple to interpret [22].

2.2. Average minimum resolution

2.2.1. Meaning

Unlike the traditional resolutions ${}^1R_s$ and ${}^2R_s$, the average minimum resolution of SOT is not arbitrary and depends on the criteria that define observed peaks. Often, one considers two peaks to be separated as observed peaks only if two maxima are present. In this case, the minimum resolution of two peaks with equal standard deviations depends on the ratio of peak heights. The average minimum resolution is the mean value of all minimum resolutions of different peak pairs, and it depends on the variation of peak heights in the separation. For the common case in which peak heights follow an exponential (or near exponential) distribution [27–32], the average minimum resolution is 0.725 [31,33–36]. However, this limiting value is correct only as the saturation approaches zero. At larger saturations, a maximum may be comprised of more than one peak (e.g., a single maximum may contain two peaks). For two multi-constituent maxima, theory shows that the two nearest-neighbor peaks – one in each maximum – have a proportionally smaller minimum interval of separation than only two peaks, because the average interval between the maxima centers increases more rapidly than the maxima widths [10,13]. This minimum interval is reduced further as the number of peaks per maximum increases. The net result is the average minimum resolution is not a constant but decreases with saturation. At any

saturation it differs with both the dimensionality of separation and the type of observed peak, as previously stated. These variations make it difficult to interpret SOT predictions at a given saturation.

The variations also mean that the 1D and 2D effective saturations, which depend on the average minimum resolution (see Eqs. (7) and (8)), do not increase at the same rate, or even at proportional rates, as saturation increases. Consequently, for observed peaks that are maxima, SOT predictions for 1D and 2D separations scale differently relative to saturation and effective saturation, leading to different interpretations of the same predictions relative to the two metrics.

The interpretations differ for a simple reason. Relative to saturation, the SOT-based peak capacity is inversely proportional to $\bar{R}_{1D}$ in 1D separations [3] and $(\bar{R}_{2D})^2$ in 2D separations [26]. Although 1D and 2D separations of the same mixture have the same SOT-based peak capacities at the same saturation, the relative sizes of the peak-capacity units differ if the average minimum resolutions differ [22]. In contrast, at the same effective saturation the assignment of unit values to ${}^1R_s$ and ${}^2R_s$ determines traditional peak capacities having units of the same relative size in both separations.

2.2.2. Calculation

The equations for the average minimum resolution of singlets in 1D separations of randomly distributed peaks are known and reported in Appendix A. Their 2D equivalents are derived here. The general expression for the average minimum resolution $\bar{R}_{2D}$ is a weighted combination of all relevant minimum resolutions [13]

$$\bar{R}_{2D} = \sum_i \sum_k p_{2D}^{ik} R_{2D}^{ik} \tag{10}$$

where p_{2D}^{ik} is the probability that two observed peaks contain i and k peaks, and R_{2D}^{ik} is the minimum resolution separating the nearest-neighbor peaks in these observed peaks. The bounds of the sums in Eq. (10) depend on the type of observed peak, whose overlap is modeled. To predict the average *total* number of observed peaks, one needs all values of i and k, i.e., the lower bounds are one and the upper bounds are infinity [13]. This is because each observed peak contributes to the observed-peak number, regardless of the number of peaks it contains. Only a subset of the i and k values is needed to predict the average number of singlets, however. A singlet is formed on separating a single peak from its nearest neighbor in any kind of observed peak, regardless of whether it is a singlet, doublet peak, triplet peak, etc. Therefore, the average minimum resolution $\bar{R}_{2D}^s$ of singlets (the symbol $\bar{R}_{2D}^s$ is distinguished from Eq. (10) by the superscript s) is obtained by setting one index (e.g., i) in Eq. (10) to unity and allowing the other index (k) to assume all values

$$\bar{R}_{2D}^s = \sum_{k=1}^{\infty} p_{2D}^{1k} R_{2D}^{1k} \tag{11}$$

The probability p_{2D}^{1k} in Eq. (11) is the conditional probability that an observed peak contains k peaks, given that the other contains only one peak. For randomly distributed peaks, this simply is the probability that an observed peak contains k peaks. This probability is the average number of observed peaks containing k peaks, divided by the average total number of observed peaks [13]

$$p_{2D}^{1k} = -(\ln p_{2D})^{-1} \frac{(1-p_{2D})^k}{k} \tag{12}$$

which is non-negative since $\ln p_{2D} = -4\alpha_{2D}$ (see Eq. (4)).

The general equation for the minimum resolution R_{2D}^{ik} depends on the specific model of overlapping peaks. In a previous paper, all observed peaks (e.g., singlets, doublet peaks, triplet peaks, etc.) in a 2D separation were modeled as maxima by the sum of partially overlapping bi-Gaussian peaks of equal height, arranged in regular hexagons resembling a cubic closest packed configuration [13]. The minimum approach between different hexagonal clusters of i and k peaks determined R_{2D}^{ik}. In spite of the model's simplicity, the R_{2D}^{ik} values so determined worked well in predicting the average total number of maxima, even for peaks having an exponential distribution of heights. The minimum resolution R_{2D}^{1k} for separating a singlet from a cluster of k peaks is obtained by assigning i the value, one, in this expression [13]

$$R_{2D}^{1k} = \frac{0.725}{2[(z_k-1)\delta/2+1]} \times \left[1 + \left\{1 + \frac{(4\delta R_{2D}^{1k})^2 (z_k^2-1)(5z_k^2+3)}{16(3z_k^2+1)} + \frac{(4\delta R_{2D}^{1k})^4 (z_k^4-1)(7z_k^2-15)}{1280(3z_k^2+1)}\right\}^{1/4}\right] \tag{13}$$

with $\delta = 2/3$ and

$$z_k = 2\sqrt{\frac{k-1/4}{3}} \tag{14}$$

In Eq. (13), the scalar δ is the average interval between the centers of nearest-neighbor peaks that overlap, divided by the peak width. The product $4\delta R_{2D}^{1k}$ is the interval between the centers of nearest neighbors in the peak cluster, divided by the peak standard deviation. The attribute z_k is the number of overlapping peaks spanning the diagonal connecting opposite vertices of the cluster. Eq. (13) states that the minimum interval between the centers of maxima formed by a singlet and a hexagonal cluster of k overlapping peaks, divided by four times the average standard deviation of these two observed peaks, equals the limiting average minimum resolution, 0.725. Eq. (13) is implicit for R_{2D}^{1k}, with R_{2D}^{1k} appearing on both sides.

With R_{2D}^{1k} solutions and Eq. (12), $\bar{R}_{2D}^s$ can be calculated from Eq. (11). A practical upper limit to k exists, because p_{2D}^{1k} approaches zero for large k (see Eq. (12)). The dependence of $\bar{R}_{2D}^s$ on saturation α_{2D} results from the dependence of p_{2D}^{1k} on α_{2D} (see Eq. (12)); in contrast, the minimum resolutions R_{2D}^{1k} are independent of α_{2D}.

3. Procedures

Eq. (13) was solved numerically for R_{2D}^{1k} using the bisection method. For different saturations α_{2D}, sufficient k values were considered, such that the probabilities p_{2D}^{1k}, Eq. (12), summed to more than 0.9999. The average minimum resolution $\bar{R}_{2D}^s$, Eq. (11), was evaluated for these α_{2D} values. The fraction of 2D peaks that are singlets, $s_{2D}/\bar{m}$, was calculated from Eq. (6) for different α_{2D} but was graphed as a function of the effective saturation $\alpha_{e,2D}$, obtained by substituting $\bar{R}_{2D}^s$ for the general expression $\bar{R}_{2D}$ in the central equation of Eq. (8).

Similar procedures were followed to determine the average minimum resolution $\bar{R}_{1D}^s$ of singlets in 1D separations, except that the 1D equivalent to R_{2D}^{1k} required solution at different saturations α_{1D} (see Appendix A). The fraction of 1D peaks that are singlets, $s_{1D}/\bar{m}$, was calculated from Eq. (5) for different α_{1D} but was graphed as a function of the effective saturation $\alpha_{e,1D}$, obtained by substituting $\bar{R}_{1D}^s$ for the general expression $\bar{R}_{1D}$ in the central equation of Eq. (7).

4. Results and discussion

Fig. 1(a) is a graph of the average minimum resolution $\bar{R}^s$ of singlets vs. the saturation α for 1D and 2D separations of randomly

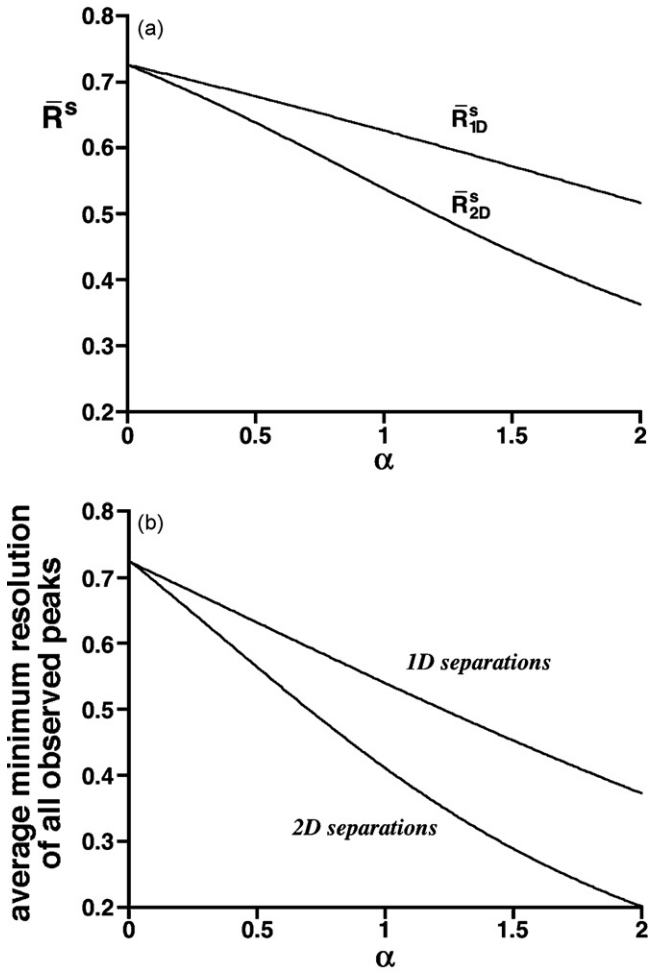

Fig. 1. Average minimum resolution vs. the saturation α for 1D and 2D separations. (a) For singlets, with average minimum resolution equal to $\bar{R}^s$. (b) For all observed peaks.

distributed peaks having an exponential distribution of heights (these distributions are assumed throughout this section). The subscripts 1D and 2D have been dropped from the axis labels, with the dimensionality of separation identified in the graph. Both $\bar{R}^s_{1D}$ and $\bar{R}^s_{2D}$ equal the limiting value, 0.725, as the saturation approaches zero. However, $\bar{R}^s_{2D}$ decreases more rapidly with increasing saturation than does $\bar{R}^s_{1D}$. The curves differ, because the ways in which peaks can overlap to form multi-constituent observed peaks, and the likelihood of peak overlap, differ in the two separation types [22]. At large saturations, the average minimum resolution is less than the minimum resolution of two peaks with equal heights and standard deviations (0.5), because the minimum resolutions separating multi-constituent maxima can be smaller [10,13]. Fig. 1(b) is the related graph of the average minimum resolution of *all* types of observed peaks vs. α. With these curves, the average *total* numbers of observed peaks in 1D and unbounded 2D separations having the same effective saturation were shown to be almost the same [22]. The curves are similar to those in Fig. 1(a) except they decrease more rapidly with α. The rapid decrease occurs because the curves include weighted contributions of minimum resolutions for all multi-constituent observed peaks, and as noted previously these minimum resolutions decrease as the number of peaks per maximum increases. Since the average minimum resolutions in Fig. 1(a) and (b) differ, the effective saturations calculated from them also differ. Therefore, it would be wrong to compare SOT predictions for 1D and 2D singlets using effective saturations calculated from the average minimum resolutions in Fig. 1(b).

Fig. 2(a) is a graph of the effective saturation α_e of singlets vs. the saturation α for 1D and 2D separations. Both curves increase rapidly with α but $\alpha_{e,2D}$ increases more rapidly. Part of this can be attributed to the geometric factor, $4/\pi$, in Eq. (8) that relates the SOT-based and usual 2D peak capacities [9,23]. However, the rates of increase are not proportional. This is because $\bar{R}^s_{2D}$ decreases more rapidly than $\bar{R}^s_{1D}$ with increasing α, as shown in Fig. 1(a). At any α, the different rates of increase cause SOT predictions to be mapped into proportionally larger values of $\alpha_{e,2D}$ than $\alpha_{e,1D}$.

Fig. 2(b) is a graph of the fraction of peaks that are singlets, $s/\bar{m}$, vs. α for 1D and unbounded 2D separations. As noted in the Introduction, this fraction decreases more rapidly for unbounded 2D separations than for 1D ones. The reason for this is clear from Fig. 1(a). Even though 1D and 2D separations of the same mixture have the same SOT-based peak capacities at the same saturation, the average minimum resolution is smaller in the 2D separation, with a peak-capacity unit of relatively smaller size. Thus it is not surprising that the 2D separation is poorer. These predictions have been published before [23] and are shown here to emphasize differences resulting from their interpretation relative to effective saturation. Fig. 2(c) is a graph of $s/\bar{m}$ vs. the effective saturation α_e for 1D and unbounded 2D separations. The ordinate $s/\bar{m}$ is the same as in Fig. 2(b), but it is graphed against α_e instead of α. In comparison to Fig. 2(b), the abscissas of a given $s/\bar{m}$ ratio are shifted to larger values, but the 2D value is shifted more because of the greater increase of α_e with α shown in Fig. 2(a). Due to these shifts, the two curves in Fig. 2(c) are now almost the same, differing by no more than 0.033 at effective saturations between 0 and 6. The agreement means that 1D and unbounded 2D separations of the same number of peaks have essentially the same number of singlet maxima, when the traditional resolutions are unity and the traditional peak capacities are the same. The agreement is valid for peak numbers up to six times larger than the traditional peak capacity. This finding is similar to that for the average total number of observed peaks [22] and strengthens the assertion that neither separation type is superior to the other. All other matters being equal, the separation with the greater traditional peak capacity (usually the 2D one) should be chosen.

The importance of the variations of $\bar{R}^s_{1D}$ and $\bar{R}^s_{2D}$ with saturation is shown in Fig. 2(d). This is another graph of $s/\bar{m}$ vs. α_e, but with the average minimum resolution determining α_e equal to the limiting value, 0.725. The curves in Fig. 2(d) are more similar than those in Fig. 2(b) because of the geometric factor, $4/\pi$. However, this factor is not enough to make the curves the same. In contrast, the curves in Fig. 2(c) are nearly the same because $\bar{R}^s_{2D}$ decreases with saturation more rapidly than $\bar{R}^s_{1D}$.

Because the average minimum resolution of singlet maxima is computed numerically, analytical equations for $s/\bar{m}$ vs. α_e do not exist. Over the range, $0 \le \alpha_e \le 6$, an excellent fit to the graphs in Fig. 2(c) is

$$\frac{s}{\bar{m}} = \frac{1}{1 + \beta_1 \alpha_e^{\beta_2} + \beta_3 \alpha_e^{2\beta_4}} \tag{15}$$

with $\beta_1 = 1.909 \pm 0.009$, $\beta_2 = 1.102 \pm 0.003$, $\beta_3 = 0.83 \pm 0.01$, and $\beta_4 = 1.453 \pm 0.005$ for 1D separations (correlation coefficient $R = 0.99999$), and with $\beta_1 = 1.961 \pm 0.009$, $\beta_2 = 1.056 \pm 0.002$, $\beta_3 = 1.076 \pm 0.009$, and $\beta_4 = 1.247 \pm 0.003$ for unbounded 2D separations ($R > 0.99999$). For $0 \le \alpha_e \le 6$, the absolute value of the maximum difference between Eq. (15) and the curves in Fig. 2(c) is 0.0040 for 1D separations and 0.0019 for unbounded 2D separations.

As previously noted, the edge effect causes an increased probability of separation near the boundary of a 2D separation. This

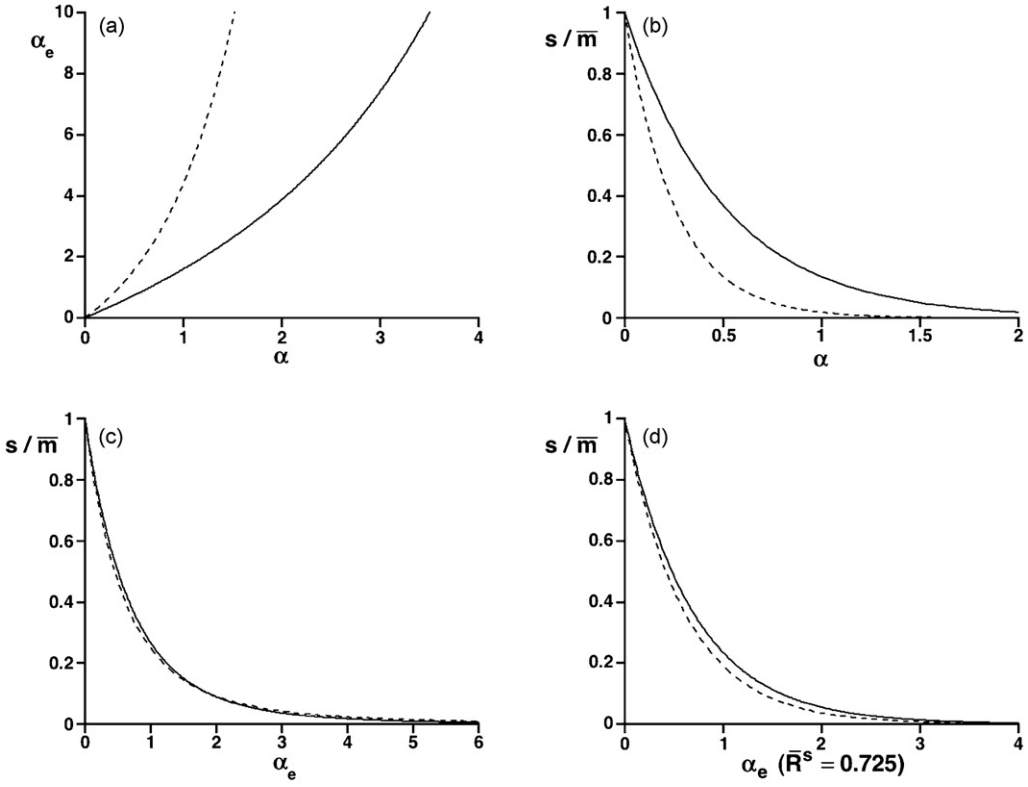

Fig. 2. SOT predictions for 1D separations (solid curves) and unbounded 2D separations (dashed curves) relative to saturation and effective saturation. (a) Effective saturation α_e of singlets vs. the saturation α. (b) The fraction of peaks that are singlets, $s/\bar{m}$, vs. α, as predicted from Eqs. (5) and (6). (c) As in (b), but with predictions of Eqs. (5) and (6) graphed against the effective saturation α_e calculated from the average minimum resolution of singlets $\bar{R}^s$ in Fig. 1(a), and Eqs. (7) and (8). (d) As in (c), but with $\bar{R}^s = 0.725$.

causes the average numbers of 2D singlets to increase beyond the predictions discussed here. The edge effect is usually small and is most important when the number of peaks is small, the saturation is high, and the peak aspect ratio is large [12]. Its effect on the $s_{2D}/\bar{m}$ ratio is not calculated here.

5. Conclusion

In this paper, the average numbers of singlet maxima in 1D and unbounded 2D separations of randomly distributed peaks having exponentially distributed heights were shown to be almost the same, when compared against effective saturation. In practice, many 2D separations contain peaks with correlated retention (or elution) times, instead of random ones. This work is still relevant because it shows that 1D and unbounded 2D separations have the same *potential* to separate singlet maxima, when their traditional peak capacities are the same. The manner in which the retention times actually are distributed is a separate issue that varies from separation to separation.

The predictions of SOT appear to be very different, when compared against saturation and effective saturation. Both predictions are valid. However, the effective saturation is the more useful metric for *comparing* separations with different average minimum resolutions. By absorbing these values into the saturation, one can use traditional peak capacities defined at unit resolution instead of SOT-based peak capacities having units of different relative size with a dependence on saturation. In this paper, separations with different dimensionalities were compared. However, other applications of effective saturation exist. For example, comparisons can be made of separations having different average minimum resolutions determined by different detection and signal-processing methods. In addition, the average minimum resolutions of 1D separations differ, when the probability density function for the interval between adjacent peaks differs [10]. Such separations can be compared at the same effective saturation.

The recognition that effective saturation is the better metric for comparing separations does not eliminate the need to know the average minimum resolution. The predictions of point-process SOT fundamentally depend on saturation, and they cannot be interpreted relative to effective saturation unless the average minimum resolution is known.

Appendix A. Average minimum resolution of 1D singlets

In a 1D separation, the average minimum resolution $\bar{R}^s_{1D}$ of singlets is the 1D analog of Eq. (11) in the main article [24]

$$\bar{R}^s_{1D} = \sum_{k=1}^{\infty} p^{1k}_{1D} R^{1k}_{1D} \tag{A.1}$$

where p^{1k}_{1D} is the conditional probability that one of two observed peaks contains k peaks, given that the other contains only one peak, and R^{1k}_{1D} is the minimum resolution separating the nearest-neighbor peaks in these observed peaks.

For randomly distributed peaks, p^{1k}_{1D} is given by the geometric distribution [24]

$$p^{1k}_{1D} = p_{1D}(1 - p_{1D})^{k-1} \tag{A.2}$$

where $p_{1D} = \exp(-\alpha_{1D})$ is the probability of separating two adjacent peaks and α_{1D} is the 1D saturation (Eqs. (3) and (1), respectively, from the main article).

For randomly distributed peaks, the minimum resolution R^{1k}_{1D} is [24]

$$R^{1k}_{1D} = \frac{0.725}{2[1 + (k-1)\gamma/2]} \left[1 + \sqrt{1 + (4\gamma R^{1k}_{1D})^2 (k^2 - 1)/12}\right] \tag{A.3}$$

where

$$\gamma = 1/\alpha_{1D} - \exp(-\alpha_{1D})/[1 - \exp(-\alpha_{1D})] \quad \text{(A.4)}$$

equals the average interval between the centers of adjacent overlapping peaks, divided by the peak width. The product $4\gamma R_{1D}^{1k}$ is the interval between adjacent peak centers in a cluster of k equally spaced overlapping peaks, divided by the peak standard deviation. The interpretation of Eq. (A.3) is similar to that of Eq. (13) from the main article, except the cluster of k overlapping peaks is linearly contiguous and not hexagonal [24]. Eq. (A.3) is implicit for R_{1D}^{1k}. The number 0.725 in Eq. (A.3) is the average minimum resolution of two peaks having an exponential distribution of heights, and it replaces 0.71 in the original Ref. [24] as a more accurate coefficient.

With R_{1D}^{1k} solutions and Eq. (A.2), $\bar{R}_{1D}^{s}$ can be calculated from Eq. (A.1). In contrast to $\bar{R}_{2D}^{s}$, $\bar{R}_{1D}^{s}$ depends on saturation α_{1D} because both p_{1D}^{1k} (Eq. (A.2)) and R_{1D}^{1k} (Eq. (A.3)) depend on α_{1D}.

References

[1] P.D. Klein, S.A. Tyler, Anal. Chem. 37 (1965) 1280–1281.
[2] K.A. Connors, Anal. Chem. 46 (1974) 53–58.
[3] J.M. Davis, J.C. Giddings, Anal. Chem. 55 (1983) 418–424.
[4] M. Martin, D.P. Herman, G. Guiochon, Anal. Chem. 58 (1986) 2200–2207.
[5] M. Martin, Proceedings of the Congrès Mesucora '91, vol. 1, 1991, pp. 3–21.
[6] F.J. Oros, J.M. Davis, J. Chromatogr. 591 (1992) 1–18.
[7] J.M. Davis, Anal. Chem. 65 (1993) 2014–2023.
[8] M.C. Pietrogrande, F. Dondi, A. Felinger, J.M. Davis, Chemom. Intell. Lab. Syst. 28 (1995) 239–258.
[9] M. Martin, Fresenius J. Anal. Chem. 352 (1995) 625–632.
[10] J.M. Davis, Anal. Chem. 69 (1997) 3796–3805.
[11] M.C. Pietrogrande, N. Marchetti, F. Dondi, P.G. Righetti, Electrophoresis 24 (2003) 217–224.
[12] J.M. Davis, J Sep. Sci. 28 (2005) 347–359.
[13] S. Liu, J.M. Davis, J. Chromatogr. A 1126 (2006) 244–256.
[14] F. Dondi, A. Bassi, A. Cavazzini, M.C. Pietrogrande, Anal. Chem. 70 (1998) 766–773.
[15] M.C. Pietrogrande, N. Marchetti, F. Dondi, P.G. Righetti, Electrophoresis 23 (2002) 283–291.
[16] A. Felinger, L. Pasti, F. Dondi, Anal. Chem. 62 (1990) 1846–1853.
[17] A. Felinger, L. Pasti, F. Dondi, Anal. Chem. 64 (1992) 2164–2174.
[18] M.C. Pietrogrande, F. Dondi, A. Felinger, J. High Resol. Chromatogr. 19 (1996) 327–332.
[19] N. Marchetti, A. Felinger, L. Pasti, M.C. Pietrogrande, F. Dondi, Anal. Chem. 76 (2004) 3055–3068.
[20] M.C. Pietrogrande, N. Marchetti, A. Tosi, F. Dondi, P.G. Righetti, Electrophoresis 26 (2005) 2739–2748.
[21] M.C. Pietrogrande, M.G. Zampolli, F. Dondi, Anal. Chem. 78 (2006) 2579–2592.
[22] J.M. Davis, P.W. Carr, Anal. Chem. 81 (2009) 1198–1207.
[23] J.M. Davis, Anal. Chem. 63 (1991) 2141–2152.
[24] J.M. Davis, J. Chromatogr. A 831 (1999) 37–49.
[25] P. Schoenmakers, P. Marriott, J. Beens, LCGC North Am. 16 (335–336) (2003) 338–339.
[26] W. Shi, J.M. Davis, Anal. Chem. 65 (1993) 482–492.
[27] L.J. Nagels, W.L. Creten, P.M. Vanpeperstraete, Anal. Chem. 55 (1983) 216–220.
[28] D.P. Herman, M.-F. Gonnord, G. Guiochon, Anal. Chem. 56 (1984) 995–1003.
[29] L.J. Nagels, W.L. Creten, Anal. Chem. 57 (1985) 2706–2711.
[30] F. Dondi, Y.D. Kahie, G. Lodi, M. Remelli, P. Reschiglian, C. Bighi, Anal. Chim. Acta 191 (1986) 261–273.
[31] M.Z. El Fallah, M. Martin, Chromatographia 24 (1987) 115–122.
[32] M.C. Pietrogrande, A. Cavazzini, F. Dondi, Rev. Anal. Chem. 19 (2000) 123–155.
[33] W.L. Creten, L.J. Nagels, Anal. Chem. 59 (1987) 822–826.
[34] M.R. Schure, J. Chromatogr. 550 (1991) 51–69.
[35] J.M. Davis, Chromatographia 42 (1996) 367–377.
[36] A. Felinger, Anal. Chem. 69 (1997) 2976–2979.

Glossary

In these symbols, the subscripts and superscripts n equal one for 1D separations and two for 2D separations

^{n}D: length or duration of nth dimension of separation
$\bar{m}$: average number of peaks (mixture constituents) in separation ensemble
$^{n}n_c$: traditional peak capacity of nth dimension of separation
$n_{c,2D}$: traditional 2D peak capacity
p_{nD}: probability of separating a peak in n-dimensional separation (from adjacent neighbor for $n = 1$; from nearest neighbor for $n = 2$)
p_{nD}^{ik}: in n-dimensional separation, probability that two observed peaks contain i and k peaks
$\bar{R}_{nD}$: general average minimum resolution in n-dimensional separation
$\bar{R}_{nD}^{s}$: average minimum resolution of singlets in n-dimensional separation
R_{nD}^{ik}: in n-dimensional separation, minimum resolution of nearest neighbors in two observed peaks containing i and k peaks
$^{n}R_s$: traditional resolution of nth dimension of separation
s_{nD}: average number of singlets in n-dimensional separation
z_k: number of 2D peaks spanning diagonal of hexagonal cluster of k peaks
α_{nD}: saturation of n-dimensional separation
$\alpha_{e,nD}$: effective saturation of n-dimensional separation
β_1–β_4: fitting coefficients in Eq. (15)
γ: average interval between centers of adjacent overlapping 1D peaks, divided by peak width
δ: average interval between centers of nearest-neighbor 2D peaks that overlap, divided by peak width
$^{n}\sigma$: peak standard deviation in nth dimension of separation